

# DESIGN AND ANALYSIS OF METAMATERIAL ABSORBERS

A DISSERTATION  
SUBMITTED IN PARTIAL FULFILLMENT OF THE REQUIREMENTS  
FOR THE AWARDS OF THE DEGREE

OF

MASTER OF TECHNOLOGY  
IN  
**MICROWAVE AND OPTICAL COMMUNICATION**

Submitted by:

**KESHAV BHATI**

(2K19/MOC/01)

Under the Supervision of

**Dr. Priyanka Jain**



Department of Electronics and Communication Engineering

DELHI TECHNOLOGICAL UNIVERSITY

(Formerly Delhi college of Engineering)

Bawana Road, Delhi-110042

JULY, 2021

## CANDIDATE'S DECLARATION

I **KESHAV BHATI**, Roll No. 2K19/MOC/01, hereby declare that the work presented in this project dissertation titled “**DESIGN AND ANALYSIS OF METAMATERIAL ABSORBERS**” which is submitted by me to the Department of Electronics and Communication, Delhi Technological University, Delhi in the partial fulfilment of the requirement for the award of the degree of Master of Technology, is original and not copied from any source without proper citation. This work has not previously formed the basis for the award of any Degree, Diploma Associateship, Fellowship or other similar title or recognition.

Place: Delhi

Date: 28/07/2021



KESHAV BHATI

---

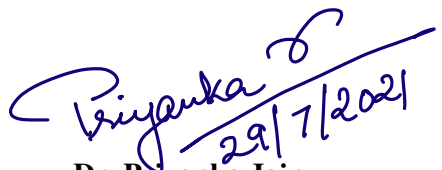
## CERTIFICATE

I hereby certify that this report titled “**DESIGN AND ANALYSIS OF METAMATERIAL ABSORBERS**” which is submitted by **KESHAV BHATI** (2K19/MOC/01) in Department of Electronics and Communication Engineering, Delhi Technological University, Delhi in partial fulfilment of the requirement for the award of the award of Master of Technology, is a record of project work carried out by the student under my supervision. To the best of my knowledge this work has not been submitted in part or full for any Degree or Diploma to this University or elsewhere.

Place: Delhi

Date: 28/07/2021

Prof. N S Raghava  
(Head of the Department,  
Dept. of Electronics and Communication  
Engineering)

  
29/7/2021  
Dr. Priyanka Jain  
(SUPERVISOR)

---

## ABSTRACT

As the communication technology is advancing at a rapid pace, demand for highly efficient devices is also growing. Metamaterials are developed as a new technology in communication, physics and material science in the recent decades, particularly in the field of microwave communication. There is a lot of research going on right now to develop metamaterial structures that can be used in developing more advanced ways of communication.

Since the introduction of metamaterials in 1968 by a *Victor Veselago* [1] by a speculation of existence of “simultaneous negative permittivity and permeability”. Since then, a tremendous amount of research in the field of metamaterials has been carried out. Metamaterials are classified as such artificial structures which have some unique properties that are not easily found in nature. Such properties are negative permittivity, negative permeability which results in negative refractive index. They are also called as double-negative media (DNG) and left-handed structure. Generally, metamaterials consist of small elements known as unit cell which are then repeated periodically to form a homogenous metamaterial. The size of the MA unit cell must be smaller than the one fourth of the resonant wavelength to achieve homogenization. It was also found out that these materials can change the behavior of electromagnetic waves in unexpected ways.

The main focus of this report is on Metamaterial absorbers. Chapter 1 gives a brief introduction about metamaterial and metamaterial absorbers along with the applications of metamaterial in filter, antennas, absorber, super lenses etc. In this chapter a brief introduction about the terminologies related to metamaterials is also given. Chapter 2 presents a review of some previous literature on metamaterial absorbers described in three sections: narrowband absorber, multiband absorber and broadband absorbers.

Chapter 3 presents the design of an ultrathin perfect metamaterial-absorber based on a dual split-ring with a cross-resonator designed on an ultrathin low cost FR4 substrate with a thickness of 1.6mm ( $0.026\lambda_0$  corresponding to the resonant frequency) and unit cell size of  $8 \times 8$  mm<sup>2</sup>. The proposed absorber has 99.99% absorptivity at 5.02 GHz in C-band. The permittivity, permeability and normalized impedance have been calculated to find the impedance matching of the proposed structure. The structure has also been analyzed by varying different design parameters. To study the effect of the rotational angle of splits the proposed structure was rotated 45° clockwise and absorption response has been analyzed, the rotated structures have multiband absorption response in X-band and Ku-band.

---

Chapter 4 presents the design of a metamaterial absorber (MA) inspired from a split-ring structure has been designed that exhibits three resonant peaks in the C-band and starting of X-band range. Proposed structure for the absorber is a three-layer rectangular split-ring with different absorption peaks at 8.488, 8.02, 7.51 GHz with 99.25%, 95.11%, 93.93% absorptivity respectively. MA is designed on the low-cost FR-4 material with dielectric constant 4.4 and substrate thickness 0.5 mm. The absorber's performance is measured in terms of three-layer absorption, material parameters, and normalized impedance.

---

## **ACKNOWLEDGEMENT**

The success and final outcome of this project require a lot of guidance and assistance from many people and I am extremely fortunate to get this all along the completion of my project work. Whatever I have done is only due to such guidance and assistance and I would not forget to thank them.

I owe my profound gratitude to my supervisor Dr. Priyanka Jain for giving an opportunity to do this work. Dr. Priyanka Jain who took keen interest on my project work and guided me all along, till the completion of my project work by providing all the necessary information, constant encouragement, sincere criticism and sympathetic attitude.

**KESHAV BHATI**

---

# CONTENTS

<b>CANDIDATE’S DECLARATION</b> .....	ii
<b>CERTIFICATE</b> .....	iii
<b>ABSTRACT</b> .....	iv
<b>ACKNOWLEDGEMENT</b> .....	vi
<b>CONTENTS</b> .....	vii
<b>LIST OF TABLES</b> .....	ix
<b>LIST OF FIGURES</b> .....	x
<b>1. INTRODUCTION</b> .....	1
1.1. BASIC OVERVIEW .....	2
1.2. TERMINOLOGIES RELATED TO METAMATERIALS .....	5
1.2.1. BACKWARD WAVES.....	5
1.2.2. LEFT-HANDED (LH) .....	7
1.2.3. ELECTROMAGNETIC BAND GAP STRUCUTURES .....	7
1.3. METAMATERIAL APPLICATIONS .....	7
1.3.1. METAMATERIAL ANTENNAS .....	8
1.3.2. METAMATERIAL FILTERS .....	8
1.3.3. METAMATERIAL SUPERLENSES .....	9
1.3.4. METAMATERIAL CLOAKS .....	9
1.3.5. METAMATERIAL AS ABSORBERS .....	10
1.3.6. MOTIVATION .....	11
<b>2. LITERATURE REVIEW</b> .....	13
2.1. NARROWBAND METAMATERIAL ABSORBERS .....	13
2.2. MULTIBAND ABSORBERS .....	14
2.3. BROADBAND ABSORBERS .....	15
<b>3. DESIGN AND ANALYSIS OF A DUAL SPILT-RING BASED METAMATERIAL ABSORBER</b> .....	17
3.1. INTRODUCTION .....	17
3.2. DESIGN AND SIMULATION .....	19
3.3. RESULTS AND DISCUSSION .....	20

---

3.4. ROTATED UNIT CELL .....	23
<b>4. DESIGN AND ANALYSIS OF RING MULTIBAND METAMATERIAL ABSORBER .....</b>	<b>28</b>
4.1. DESIGN AND SIMULATION .....	28
4.2. PARAMETRIC ANALYSIS .....	35
<b>5. CONCLUSION .....</b>	<b>36</b>
5.1. CONCLUSION .....	37
<b>6. FUTURE SCOPE .....</b>	<b>39</b>
<b>LIST OF PUBLICATION .....</b>	<b>40</b>
<b>REFERENCES .....</b>	<b>41</b>

---



## LIST OF TABLES

TABLE -3.1: Design parameters of the proposed unit cell

TABLE - 3.2: Absorptivity results w.r.to different ring width

TABLE - 3.3: Absorptivity results w.r.to different outer ring split size

TABLE - 3.4: Comparison of MA structure with different angle of rotation

TABLE - 3.5: Comparison of the proposed work with previous works

TABLE - 4.1: Design Parameters of the unit cell

TABLE - 4.2: Length and size of metal loops

TABLE - 4.3: Absorptivity results with different numbers of slots

TABLE – 4.4: Absorptivity results with different slot size

---

---

## LIST OF FIGURES

Fig. 1.1.  $\epsilon - \mu$  diagram

Fig. 1.2. Direction of  $S$  and  $\beta$  in (a) Right-handed materials (b) Left-handed materials

Fig. 1.3. (a) Wave propagation in (a) RH medium (b) LH medium

Fig. 1.4. (a) Forward wave supporting RH transmission line (b) Backward wave supporting LH transmission line

Fig. 1.5. Dispersion diagram of (a) Forward wave (b) Backward wave

Fig. 1.6. Metamaterial based antennas

Fig. 1.7. Metamaterial Super lens

Fig. 3.1. (a) Simulation setup of the unit cell (b) Schematic diagram of the MA

Fig. 3.2. (a) Three-dimensional geometrical model of the unit cell, (b) Simulated absorptivity plot under normal incidence and TE polarization.

Fig. 3.3. Simulated results of (a) effective permittivity, (b) effective permeability and (c) Normalized impedance

Fig. 3.4. Simulated Absorptivity results (a) for different incidence angle under TE polarization and (b) for different polarization angle under normal incidence.

Fig. 3.5. Simulated Absorptivity variation w.r.to variation of (a) circular ring width and (b) outer ring split gap size

Fig. 3.6. (a) Proposed unit cell structure after  $45^\circ$  rotation, (b) simulation setup of the unit cell

Fig. 3.7. Simulated Absorptivity response of the rotated unit cell

Fig. 3.8. Simulated results of (a) Permittivity and permeability (b) Normalized Impedance

Fig. 3.9. Simulated Absorptivity of rotated structure (a) for different polarization angle under normal incidence and (b) for different incidence angle under TE polarization

Fig. 4.1. Geometry of three-layer MA unit Cell

---

Fig. 4.2. Plot of S11 w.r.to frequency (GHz)

Fig. 4.3. Absorptivity result of MA unit cell

Fig. 4.4. Geometry of a 3-layer MA with a slot on top layer

Fig. 4.5. Plot of S11 vs frequency of MA unit cell with one slot

Fig. 4.6. Absorption result of the MA unit cell with a slot

Fig. 4.7. Geometry of MA unit cell with 2 slots in layers

Fig. 4.8. Absorption plot of unit cell with slots in the middle and top layer

Fig. 4.9. Geometry of (a) three-layer split ring MA unit cell (b) Top view of the unit cell

Fig. 4.10. Absorptivity result of split ring MA unit cell.

Fig. 4.11. Simulated results of reflectivity and absorptivity of split-ring unit cell.

Fig. 4.12. Comparison of absorptivity of all structures

Fig. 4.13. Absorptivity variation with variation of slot size

---

# **CHAPTER - 1**

## **INTRODUCTION**

---

## 1.1. BASIC OVERVIEW

A new kind of artificial materials known as metamaterials has developed as a new technology in the field of microwave communication during the previous few decades. Metamaterials have piqued the interest of researchers due to their novel application and remarkable characteristics that are not typically seen in nature.

The history of metamaterials began in 1968, when a Russian scientist named *Viktor Veselago* hypothesized the possibility of “substances having simultaneous negative values of permittivity ( $\epsilon$ ) and permeability( $\mu$ )” [1]. It was further investigated by *Pendry et. al.* [2] in late 90’s, in which he proposed negative- $\epsilon$ /positive- $\mu$  and positive- $\epsilon$ /negative- $\mu$  structures. Smith et al. [3] demonstrated the first microwave experiments.

Since, most of the naturally occurring materials exhibit positive values of permittivity( $\epsilon$ ) and permeability( $\mu$ ), they are classified as Double Positive (DPS) materials. Metamaterial (MTM) are defined as artificial electromagnetic structures with unusual properties not readily found in nature. Metamaterials are engineered from assemblies of artificial structures or unit cells of dimensions much smaller than the operating wavelength. The average unit cell size must be less than the quarter of wavelength ( $p < \lambda/4$ ). These unit cells are organized in a regular pattern and show electromagnetic characteristics not often observed in nature. [1]. Those properties are simultaneous negative permittivity ( $\epsilon$ ) and permeability ( $\mu$ ), that results into negative refractive index ( $\eta$ ); since,

$$\eta = \pm \sqrt{\epsilon_r \mu_r} \quad (1.1)$$

where,  $\mu_r$  and  $\epsilon_r$  are permeability and permittivity respectively and  $\eta$  is refractive index. Based on the sign of  $\epsilon_r$  and  $\mu_r$ , there are four combination in the pair ( $\epsilon$ ,  $\mu$ ) i.e. (+,+), (-,+), (-,-), and (+,-) as depicted in the  $\epsilon$ - $\mu$  diagram of Fig 1. The first 3 combinations are well known as conventional material. In the last combination (in third quadrant) with simultaneous negative  $\epsilon$  and  $\mu$  are double negative (DNG) materials also known as Left-handed (LH) materials.

The first Quadrant( $\epsilon > 0$ ,  $\mu > 0$ ) represents right-handed material or Double positive structure (DPS). Forward wave propagation occurs in the material in the first quadrant. These are the most commonly used materials and follows right-hand thumb rule for the direction of wave propagation.

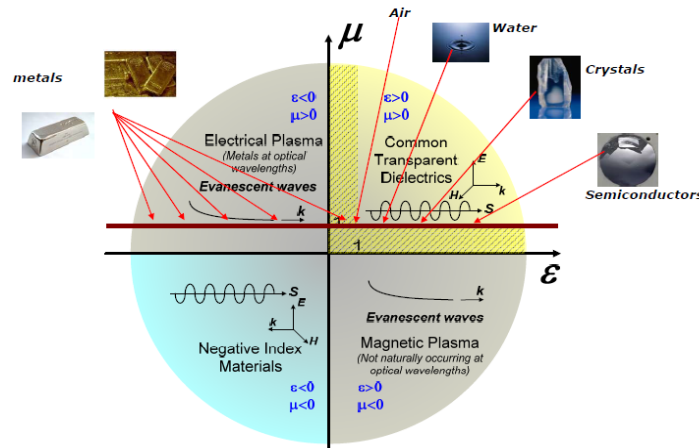


Fig. 1.1.  $\epsilon - \mu$  diagram

The second Quadrant covers Epsilon negative (ENG) medium, these mediums have permeability greater than zero & permittivity less than zero ( $\mu > 0$ ,  $\epsilon < 0$ ). In certain frequency ranges many plasmas exhibit this characteristic. At optical frequencies Silver, gold and aluminum exhibit negative- $\epsilon$ . An array of infinitely long thin metallic wires also shows this characteristic.

The fourth quadrant ( $\epsilon > 0$  and  $\mu < 0$ ) corresponds to the  $\mu$  negative materials or MNG. At radio-frequencies, there is a class of gyrotropic natural materials with a negative real part of the permeability. Split-ring structures also shows this behavior.

The third-quadrant ( $\epsilon < 0$  and  $\mu < 0$ ) represents Metamaterials also called as Left-handed materials or Double Negative material (DNG), negative index materials or backward wave media. The left-handed rule applies to these materials because wave propagation occurs in the backward direction in the medium, as opposed to the forward direction in the DPS media. Due to negative value of  $\epsilon$  and  $\mu$  the refractive index of the medium ( $\eta$ ) is also negative. Various ENG and MNG structures combined together can exhibit DNG behavior.

Metamaterials found their application in the field of microwave filters, super lenses, invisibility cloaks, antennas, sensors and electromagnetic absorbers. Electromagnetic properties of the metamaterial devices depend on the dimensions and geometry of the unit cell and these properties may be changed by altering the size, dimension, shape and configuration of the unit cell. As a consequence, material characteristics like permittivity and permeability may be controlled.

Double negative (DNG) materials are also known as left-handed materials because they follow left-hand rule of wave propagation instead of right-hand rule. The

immediate result of negative  $\epsilon$  and  $\mu$  in metamaterials is we get a left-handed triplet of electric field  $E$ , magnetic field  $H$  and propagation constant ( $\beta$ ) when we change the sign of  $\epsilon$  and  $\mu$  in the four Maxwell's equations. This implies that the propagation constant ( $\beta$ ) and the group velocity or Poynting vector ( $S$ ) are anti-parallel to each other or in the opposite direction. Metamaterials behave in the opposite way to conventional or right-handed materials (RHM), which have  $S$  and  $\beta$  pointing in the same direction. This results in the backward wave propagation in the LHM which is another unique property of metamaterials.

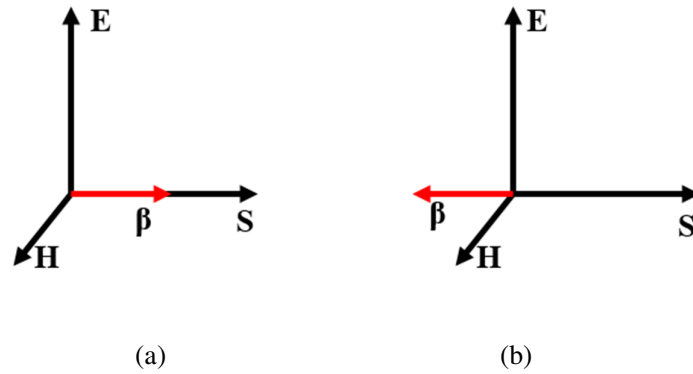


Fig. 1.2. Direction of  $S$  and  $\beta$  in (a) Right-handed materials (b) Left-handed materials

Maxwell's equations can be used to elaborate the above theory. Now, consider a lossless media in regions without sources. Now, in case of right-handed (RH) medium, where  $\epsilon, \mu > 0$ , we can write;

$$\beta \times E = +\omega\mu H \quad (1.2)$$

$$\beta \times H = -\omega\epsilon E \quad (1.3)$$

As illustrated in Fig. 1.2(a), the above equations form the well-known right-handed triad ( $E, H, \beta$ ). In the case of Left-Handed medium ( $\epsilon, \mu < 0$ ), we may write,  $|\epsilon| = -\epsilon > 0$  and  $|\mu| = -\mu > 0$

$$\beta \times E = -\omega|\mu|H \quad (1.4)$$

$$\beta \times H = \omega|\epsilon|E \quad (1.5)$$

Phase velocity varies inversely with  $\beta$  and can be given by,

$$v_p = \omega / \beta \quad (1.6)$$

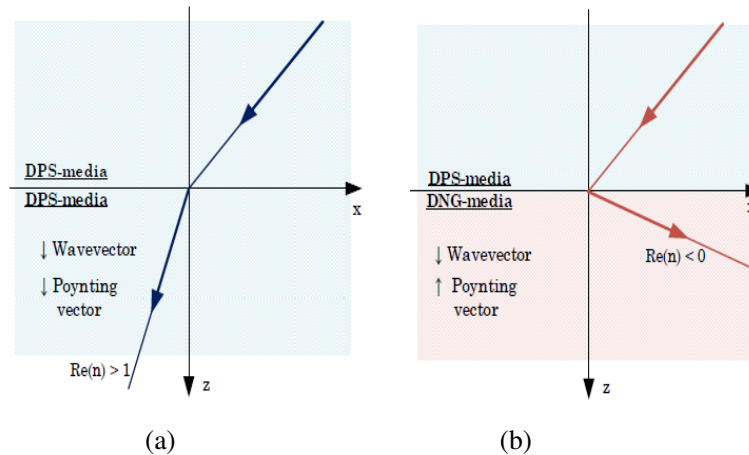


Fig. 1.3. (a) Wave propagation in (a) RH medium (b) LH medium

As a result, the phase velocity in an LH media is the opposite of that in a RH medium, since  $\beta$  is positive in a RH medium (outward propagation from the source) and negative in an LH medium (inward propagation to the source) [4]. Phase, which is related to phase velocity ( $v_p$ ), propagates backward to the source in the opposite direction as power, which is related to group velocity in a Left-handed medium ( $v_g$ ). Thereby, the waves flow in a so-called backwards fashion (i.e., the wave phase appears to undulate backwards while the energy propagates along the incident in a forward direction).

## 1.2. TERMINOLOGIES RELATED TO METAMATERIALS

### 1.2.1. BACKWARD WAVES

This term refers to the existence of the antiparallel phase and group velocities, well known in conventional materials but fails to inform on the material nature of LH MTM [4]. The phase velocity ( $v_p$ ) is associated with carrier wave and the envelope or wave form travels with the group velocity ( $v_g$ ). Carrier wave and envelope have different velocities in a dispersive medium. The waves might be forward or backward wave depending on the nature of the dispersion [5]. Forward waves were formed when the medium has normal dispersion i.e., both  $v_p$  and  $v_g$  are in the same direction. However, in anomalous dispersive medium, the backward waves were formed since the phase velocity ( $v_p$ ) and group velocity ( $v_g$ ) are in the opposite directions. As a result, backward waves are merely a common occurrence in dispersive propagation [5-6].



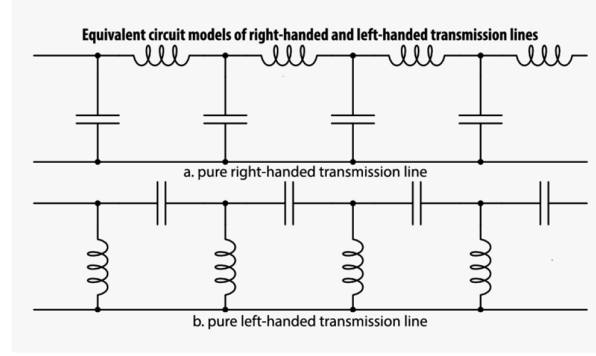


Fig. 1.4. (a) Forward wave supporting RH transmission line (b) Backward wave supporting LH transmission line

Fig. 1.4 shows the transmission line equivalent of forward and backward supporting waves respectively. There is shunt capacitance and series inductance in the forward line, but no resistive losses as shown in Fig. 1.4(a). It represents a low pass filter type LC line. Here,  $Z=j\omega L$  and  $Y=j\omega C$ , since  $\gamma = j\beta = \pm \sqrt{ZY}$ ,  $\beta = \omega\sqrt{LC}$  [6]. When  $\omega$  is plotted as a function of  $\beta$ , as shown in Fig. 1.5(a) it is a straight line of constant slope.

$$v_p = \omega/\beta = 1/\sqrt{LC} \quad (1.7)$$

$$v_g = d\omega/d\beta = \omega/\beta = 1/\sqrt{LC} \quad (1.8)$$

therefore,  $v_p = v_g$ , representing forward wave.

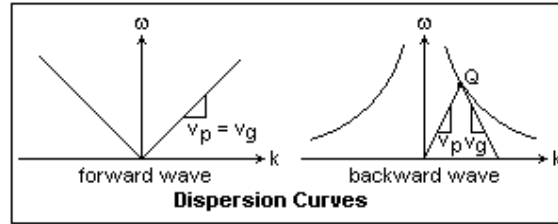


Fig. 1.5. Dispersion diagram of (a) Forward wave (b) Backward wave

The backward wave line is shown in Fig. 1.5(b). It is a high-pass line with shunt inductance and series capacitance. Here,  $Z = 1/j\omega C$  and  $Y = 1/j\omega L$ . Also,  $\gamma = j\beta = \pm \sqrt{ZY}$ ,  $\beta = 1/\omega\sqrt{LC}$ . This gives the dispersion relation of backward wave support in line.

$$v_p = \omega/\beta = \omega^2/\sqrt{LC} \quad (1.9)$$

$$v_g = d\omega/d\beta = \omega/\beta = -\omega^2/\sqrt{LC} \quad (1.10)$$

Thus, phase and group velocity are in opposite direction to each other i.e.,  $v_p = -v_g$ . These kinds of waves are known as backward waves.

### **1.2.2. LEFT-HANDED (LH)**

This term is originally suggested by *Veselago* [1]. Metamaterials are also referred as left-handed materials because they follow left-hand rule of wave propagation instead of right-hand rule. When we change the sign of  $\epsilon$  and  $\mu$  in the four Maxwell's equations, we get a left-handed triplet of electric field  $E$ , magnetic field  $H$ , and propagation constant ( $\beta$ ), which is an immediate result of negative  $\epsilon$  and  $\mu$  in metamaterials. This implies that the propagation constant ( $\beta$ ) and the group velocity or Poynting vector ( $S$ ) are anti-parallel to each other or in the opposite direction.

### **1.2.3. ELECTROMAGNETIC BAND GAP STRUCTURES**

Electromagnetic bandgap (EBG) structures are made up of periodic metal patches on a dielectric substrate. EBG structures can also be created using solely dielectric materials. EBG structures have the property of preventing surface wave propagation in a certain frequency band while simultaneously reflecting any incident EM wave with no phase shift. The features of EBG structures mentioned above can be exploited to improve the characteristics of an antenna [7-8]. The EBG surface has the following interesting features:

- a. In a continuous RF spectrum, an alternate passband-stopband can be created using EBG structures, which were also helpful for making of filters and other components.
- b. Slow-wave propagation is suppressed, which is beneficial for developing small, miniaturized microwave devices.
- c. Supporting the propagation of backward waves. It contributes to the development of transmission line-based metamaterials.

## **1.3. METAMATERIAL APPLICATIONS**

Metamaterials may be integrated with conventional electronics devices and one can change the electromagnetic behavior of EM waves simply by manipulating their form, size, orientation, geometry, and arrangement. This provides benefits that are beyond the scope of conventional materials. Metamaterials found their application in the field of

---

microwave filters [9-10], super lenses [11], invisibility cloaks [12], antennas [13-14] and electromagnetic absorbers [15-24].

### 1.3.1. METAMATERIAL ANTENNAS

Metamaterials can be utilized to increase the performance of the small size patch antennas systems. Various properties and shortcomings of patch antennas such as boosting radiation efficiency, miniaturization the substrate of printed metamaterial antennas, reducing radiator size, improving antennas bandwidth can be improved and enhanced by using metamaterials with antennas also enabling multiband operations.

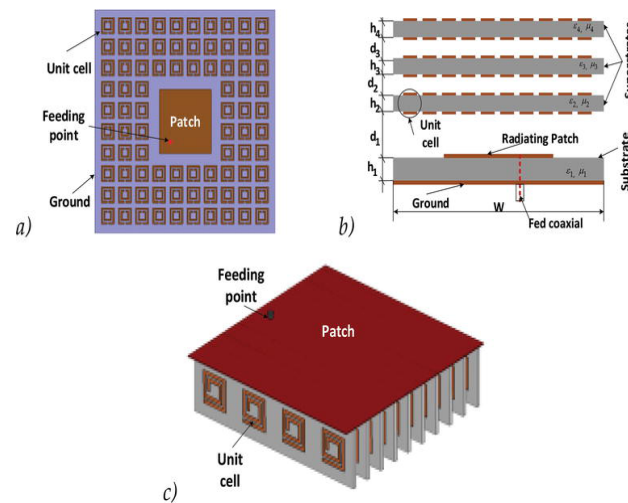


Fig. 1.6. Metamaterial based antennas

To increase their radiation and matching performance, metamaterial coatings are applied to electrically small electric and magnetic dipole-antennas. A patch antenna's gain, bandwidth, and return loss can all be improved by using metamaterials. Communication linkages, navigation systems, surveillance sensors, and command and control systems can all benefit from metamaterial antenna systems.

### 1.3.2. METAMATERIAL FILTERS

The metamaterial-based filters are resonant-type metamaterial transmission lines, which combines sub-wavelength resonators together with other elements like shunt inductances or series capacitances, load a host transmission line. This can obtain a propagating medium with controllable characteristics [9]. One, two, or many sub-wavelength resonator unit cells may be used in these structures. Metamaterials can be used in designing filters, this offers many advantages like sharp roll off, compact size, multiple frequency operations and high out of band rejection levels.

### 1.3.3. METAMATERIAL SUPERLENSES

All natural-material lenses available today are incapable of focusing light onto an area smaller than the square of the wave length of the light used to use it, this is also known as the diffraction limit. Only propagating waves can be focused by a typical conventional lens. As a result, the picture of the object is imperfect. Because of the substantial attenuation these waves experience while travelling from the object to the image, the finer spatial details of the object (smaller than a wavelength) transmitted by the evanescent waves were lost. The origin of the diffraction limit is the loss of the evanescent spectrum.

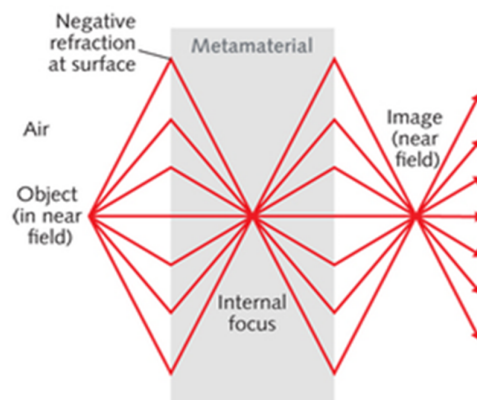


*Fig. 1.7. Metamaterial Super lens*

The decaying evanescent waves emanating from the source at the image plane are regenerated by a metamaterial-based super lens by supporting growing evanescent waves thus a Metamaterials-based lenses provides perfect imaging. As a result, the resolution of lens is considerably improved. With a perfect, flat lens based of metamaterials, sub-wavelength resolution or focusing beyond the diffraction limit is achievable. As a result, such lenses are often referred to as "super" lenses. The evanescent fields are increased within a super lens, but they will decay away from the lens.

### 1.3.4. METAMATERIAL CLOAKS

A cloak has the ability to deflect electromagnetic beams in such a way that they flow around an object with minimal distortion, giving the impression that there is nothing at all. The use of metamaterials in an invisibility cloak is known as metamaterial cloaking. This is done by changing the pathways that electromagnetic waves take as they pass through a novel cloak material.

### 1.3.5. METAMATERIAL AS ABSORBERS

Metamaterial absorbers (MA) are such metallic structure which can limit the reflection and transmission of the electromagnetic (EM) wave within a specific range of frequencies. To absorb significant electromagnetic radiations, a metamaterial absorber manipulates the loss component of the metamaterial's permittivity and permeability. Metamaterial absorbers consists of  $n \times n$  periodic array of a unit cell. In 2008, Landy et al. introduced the first metamaterial absorber [15]. When electromagnetic wave strikes the surface of the absorber, they can be transmitted, reflected, absorbed or scattered. If we assume that there is no scattering because of roughness, the absorbance may be calculated as:

$$A(\omega) = 1 - R(\omega) - T(\omega) \quad (1.11)$$

Here,  $R(\omega)$  is Reflectance which is obtained from  $|S_{11}|^2$  and  $T(\omega)$  is Transmittance derived from  $|S_{21}|^2$ . To completely absorb the impinging electromagnetic radiation, the reflectance ( $R(\omega)$ ) and transmittance ( $T(\omega)$ ) must be equal to zero. Now, to get transmittance ( $T(\omega)$ ) equals to zero, most common method is to coat the bottom side of the MTM structure is completely with a metal (generally copper), which restricts the further propagation of the wave ( $|S_{21}|^2 = 0$ ) because an electromagnetic wave cannot propagate through a metal. The reflectivity is related to the relative permittivity ( $\epsilon_r$ ) and permeability ( $\mu_r$ ). Now, to get unity absorbance, the reflectivity should be minimum or ideally it should be zero. Further the Absorbance equations will modify into:

$$A(\omega) = 1 - |S_{11}|^2 \quad (1.12)$$

To obtain equal values of  $\epsilon_r$  and  $\mu_r$ , one has to carefully choose the dimension of a metamaterial unit cell. For equal values of  $\epsilon_r$  and  $\mu_r$ , the structure's input impedance becomes equals that of empty space, which is 377 ohms. Since,

$$Z = \sqrt{\frac{\mu_0 \mu_r}{\epsilon_0 \epsilon_r}} \quad (1.13)$$

As a result of the impedance matching that occurs between the free-space and the absorber structure, waves do not reflect back off the absorber's surface. In order to achieve near-perfect absorption, the impedance matching criteria must be met and to get that the effective permittivity and permeability should be equal. Because no natural

material can meet these requirements, artificially created structures, also known as metamaterials, must be examined. By modifying the dimensions, orientation and size of the unit cell, the electromagnetic properties of a wave can be intentionally altered by modifying the structure's characteristics in terms of macroscopic factors like permittivity and permeability.

#### **1.4. MOTIVATION**

As the demand for advanced wireless communication and devices increased exponentially in the recent years, the requirement for highly efficient and miniaturized devices has also increased especially in areas of wireless communication, aircrafts, military technologies, satellite communication etc. Different technologies and methods evolved in the recent decades to overcome challenges associated with advanced communications, metamaterials were one of them.

Metamaterials are new structures that function by changing the structure's electromagnetic characteristics, such as permeability and permittivity. Due to their unusual properties beyond the scope of conventional materials, metamaterial has become an active topic of research. They offer various advantages over conventional materials such miniaturization, high efficiency, high gain etc.

Use of metamaterials structures as electromagnetic absorbers to absorb the EM wave is a wide area of research. Conventional absorbers such as Jaumann and Salisbury screen absorber are very bulky in nature but stealth technology and radar systems demand absorbers to be compact and light weight, that's where metamaterial absorbers offer an advantage due to their ultrathin thickness with near perfect absorption.

---

# **CHAPTER - 2**

## **LITERATURE REVIEW**

---

## 2. LITERATURE REVIEW

Since when the Victor Veselago [1] first speculated on existence of “substances with simultaneously negative values of permittivity( $\epsilon$ ) and permeability( $\mu$ )” and first ever metamaterial was developed by Smith et. al [3], metamaterial become a hot topic of research and numbers of research papers, letter and publication have been published in the recent years. Since the introduction of first metamaterial absorbers in 2008 [15] various narrowband, multiband and broadband absorbers have been reported in literature. Metamaterial found their applications in various domains electromagnetic absorbers is one of them.

Metamaterial absorbers are such electromagnetic absorbers which restricts the transmission and reflection of the incident electromagnetic waves in a particular frequency range. They are generally made from assemblies of metamaterial unit cell repeated periodically. Metamaterial absorbers provide advantage over conventional absorbers because of their exceptional properties and ultrathin nature.

### 2.1. NARROWBAND METAMATERIAL ABSORBERS

In 2008, first ever “perfect metamaterial absorber” was proposed by Landy et al. [15] as shown in Fig. 2.1(a). In the structure, there is an Electric Ring Resonator (ERR) on the top surface and a cut metallic wire on the bottom surface of an FR4 substrate. As the electromagnetic wave strikes the surface electric and magnetic resonance takes place at 11.65 GHz. However, it was discovered that the bottom cut wire design causes some transmission, which may be prevented by fully laminating the bottom surface with metal.

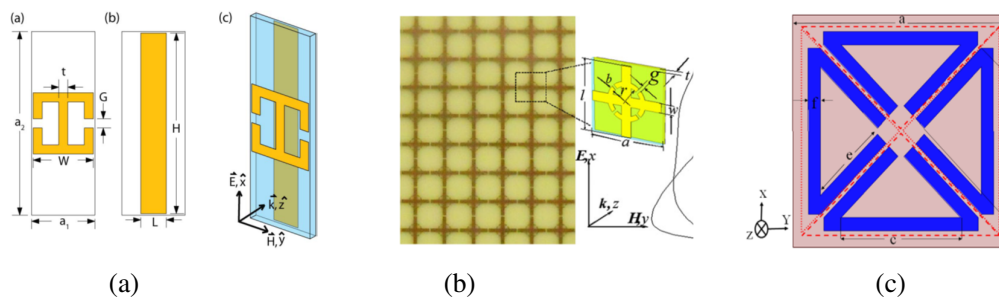


Fig. 2.1. Narrowband Absorbers

Cheng et al. [26] proposed a polarization insensitive metamaterial (MM) absorber as shown in Fig. 2.1(b) composed of a split-ring cross resonator (SRCR) on



top surface of dielectric substrate and continuous metal film on the bottom surface. The absorber has near unity absorptivity of about 99% at around 10.91 GHz. The absorber is fabricated on FR4 (lossy) substrate of only 0.4 mm thickness. In addition, in [27], a flower-shaped metamaterial absorber is employed in a two-element multiple-input-multiple-output (MIMO) system to provide excellent isolation between two patch antennas operating at 5.5 GHz which is used in WiMAX applications. The said absorber shows 98.7% absorptivity at 5.5 GHz. Also, a four-fold symmetrical structure was proposed in [30] as shown in Fig. 2.1(c) which shows an absorptivity of 99.6% at 8.65GHz.

## 2.2. MULTIBAND ABSORBERS

Several approaches are employed to demonstrate multi-frequency absorption such as the use of multiple metallic structures they can be rotated or scaled structures in a single geometry that have different resonance frequencies and also generations of some higher order modes. The use of multiple structures and multilayer structure increase the unit cell size. Therefore, for multi-frequency absorption a single structure is embedded with multiple structures (with different resonant frequencies) is preferable to other techniques.

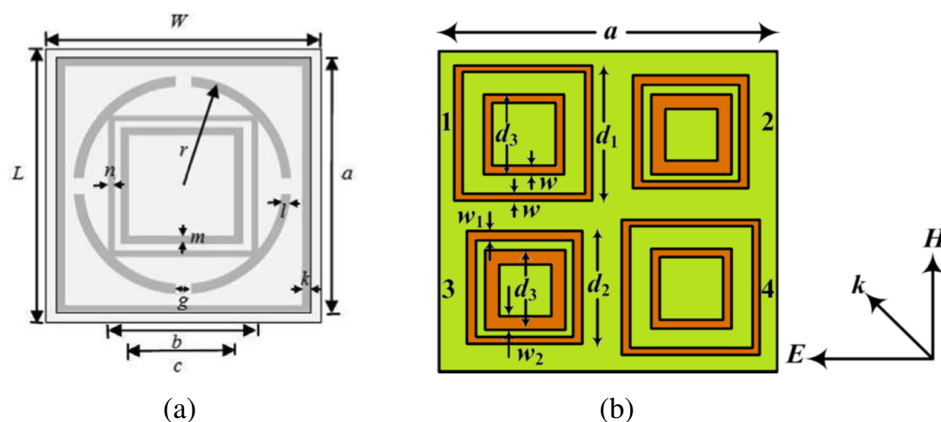


Fig. 2.2. Multiband Absorbers

In [21] authors have proposed a novel penta-band metamaterial absorber with five resonant absorption peaks with absorptivity ranging from 93% to 99.59% in between S-band to K<sub>u</sub>-band. The structure shown in Fig. 2.2(a) consists of multiple square split rings along with a circular split ring, the design of the structure is said to

have fourfold symmetry. In [31] provides a triple band absorptivity response peaks at with absorptivity from 90.7% to 97.1%.

### 2.3. BROADBAND ABSORBERS

Broadband absorbers function over a large frequency range. In the literature, many broadband absorber structures have been proposed. The most common approach for broadband absorption is the use of multi layered structures, as well as the use of several scaled copies of the same shape on a single unit cell.

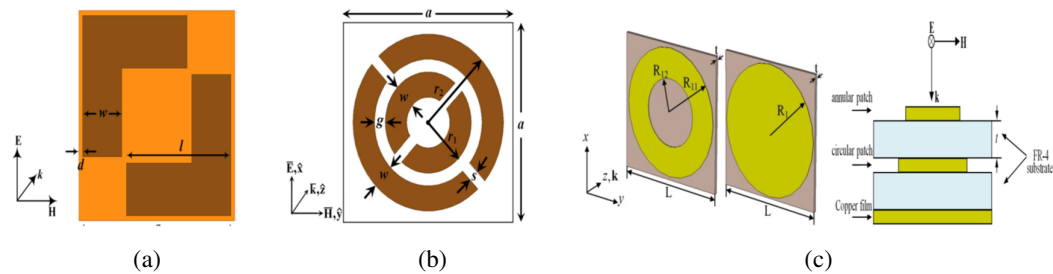


Fig. 2.3. Broadband Absorbers

S. Bhattacharya et. al [23] proposed an L-shaped ultra-thin metamaterial absorber with patches placed diagonally at the top surface shown in Fig. 2.3(a). The structure is said to have a broadband absorption response ranging from 4.6 to 7.2 GHz with greater than 90% absorptivity. It is only a single-layer structure in contrast to conventional multilayer structure. In [24] a double concentric split-rings structure which consist of two circular split-rings with their perpendicular to each other has been proposed as shown in Fig. 2.3(b) with absorption bandwidth ranging from 7.85 GHz to 12.25 GHz covering the entire X-band. In [25] authors have presented a multi-layer broadband absorber as shown in Fig. 2.3(c) showing absorption bandwidth between 8.8 GHz to 10.8 GHz.

**CHAPTER - 3**

**DESIGN AND ANALYSIS OF A DUAL  
SPLIT-RING BASED METAMATERIAL  
ABSORBER**

---

---

### 3. DESIGN AND ANALYSIS OF A DUAL SPLIT-RING BASED METAMATERIAL ABSORBER

#### 3.1. INTRODUCTION

Recently, metamaterials have become an important area of research because of their extraordinary properties and compactness [16-17]. They found their application in the field of microwave filters, super lenses, invisibility cloaks, antenna and electromagnetic absorbers. Metamaterial absorbers (MA) are such metallic structure which can limit the reflection and transmission of the electromagnetic (EM) wave within a specific range of frequencies [3]. Conventional electromagnetic absorbers such as Jaumann and Salisbury screen absorber are very bulky in nature but stealth technology and radar systems demand absorbers to be compact and light weight, that's where metamaterial absorbers offer an advantage due to their ultrathin thickness with near perfect absorption [19].

In 2008, *Landy et al.* introduced the first ever metamaterial absorber [15], since then narrowband [20], multiband [21-22] and broadband absorbers [23-25] are the hot topic for researchers.

Generally, metamaterial absorbers (MA) consist of a  $n \times n$  array of a unit cell. On top is a metallic patch and on bottom is a metallic ground, separated by a dielectric substrate [24]. The electric response is obtained at the resonance frequency by the electric field stimulation of the top metallic frequency selective surface (FSS), and magnetic fields excites the dielectric substrate, which creates an antiparallel surface current on both sides of the dielectric surface. [24]. These electromagnetic fields can manipulate the homogenized structure's effective material characteristics, causing the structure's effective permittivity and permeability to equalize at certain frequencies. [15]. As a consequence, the structure's input impedance is equal to the free space impedance, reducing absorber reflection.

A ultrawide band ultrathin MA based on circular split ring has been proposed by *S. Ghosh et al.* [24], from 7.85 to 12.25 GHz covering the entire X-band. *Yongzhi Cheng et al.* [26] proposed a polarization independent MA based on split-ring cross resonator with near unity absorptivity at around 10.91 GHz. In another work a flower shape metamaterial absorber is used to increase the isolation between the MIMO

---

**TABLE - 3.1***Design Parameters of the unit cell*

Parameters	R	r	g	w	x	a	b	h	L
Unit (mm)	3.2	2	0.3	0.8	1	0.5	0.4	1.6	8

antennas [27]. In [28] metamaterial absorber has been proposed for radar cross section (RCS) reduction as well as improving the isolation between element MIMO-antenna for Radiolocation and Aeronautical Radio Navigation Application.

The proposed structure is a single layer ultrathin metamaterial absorber (MA) based on a dual split-ring cross-resonator (DSRCR), which shows 99.99% absorption at around 5.02 GHz in C-band. The proposed structure consists of two concentric split-rings embedded with a cross metallic strips which acts as cross resonator to form a continuous metal strip. All the structure's geometrical dimensions have been tuned to get structure's absorption response close to unity. The design of the structure was analyzed for oblique incident angles ( $\Theta$ ) and by varying polarization angles ( $\phi$ ) under normal incidence. The permittivity ( $\epsilon_{\text{eff}}$  and  $\mu_{\text{eff}}$ ) of the structure have also been illustrated. Normalized impedance ( $Z_{\text{nor}}$ ) has also been calculated to know the impedance matching of the proposed absorber with the free space. The width of outer circular ring and the size of the gap in the outer ring has been varied to observe their effect on absorption response. Further, the proposed structure has been rotated 45° clockwise to observe the effect of rotational angle of the splits of circular rings. Comparing to the previous work on metamaterial absorbers, the proposed structure offer advantages such as ultrathin nature, miniaturization, near-unity absorptivity and excellent impedance matching.

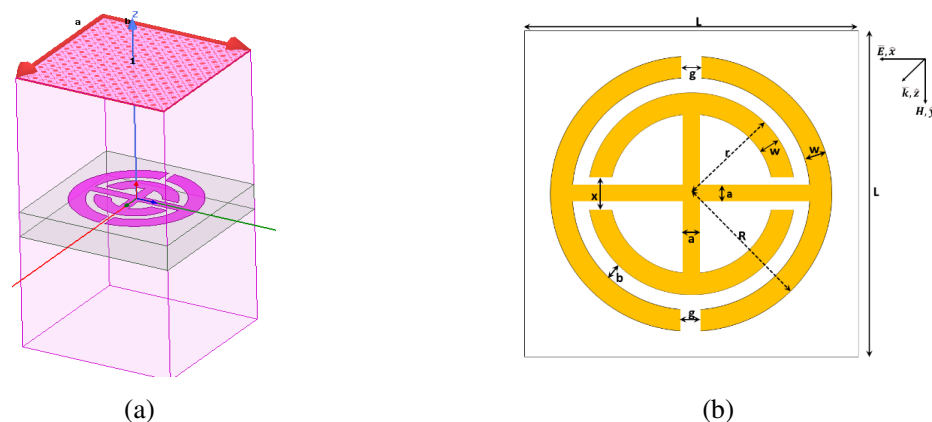


*Fig. 3.1. (a) Simulation setup of the unit cell (b) Schematic diagram of the MA*

### 3.2. DESIGN AND SIMULATION

The proposed MA unit cell as shown in Fig. 3.1 consist of single layer structure based on double split-ring cross resonator (DSRCR) and a ground metallic plane. The unit cell is made from a low-cost FR-4 substrate with a dielectric constant ( $\epsilon_r$ ) of 4.4 and a loss-tangent ( $\delta$ ) of 0.02 and a thickness of 1.6 mm. The metallic ground plane is at the bottom of the substrate, and the metallic patch is on top of it.. The metal used here is copper. The top metallic patch consists of two split rings and cross resonator metallic strip. The splits of the outer and inner ring are orthogonal to each other. The MA structure is simulated with Floquet Port and periodic boundary conditions in Ansys HFSS.

To absorb the electromagnetic radiation, a metamaterial absorbs, controls the loss components of the metamaterial, relativpermittivity ( $\epsilon_r$ ) and permeability ( $\mu_r$ ) [26]. The absorbance (A) of a surface can be given as:

$$A= 1 - R- T \quad (3.1)$$

Here,

R is Reflectance which is obtained from  $|S_{11}|^2$

T is Transmittance derived from  $|S_{21}|^2$

Since in the proposed structure, the substrate's bottom surface is completely coated with the copper, it further restricts the propagation of wave, which indicated that transmittance i.e.,  $|S_{21}|^2 = 0$ . Therefore, Eq. (3.1) can be rewritten as:

$$A(\omega) = 1 - |S_{11}|^2 \quad (3.2)$$

Because metasurfaces and metamaterials are better defined in terms of surface susceptibilities, the simulated of reflection coefficient ( $S_{11}$ ) can be used to calculate electric susceptibilities ( $\chi_{es}$ ) as given in Eq. (3.3) and magnetic susceptibilities ( $\chi_{ms}$ ) as given in Eq.(3.4). Since, there is relationship between  $\chi_{es}$  (or  $\chi_{ms}$ ) and  $\epsilon_{eff}$  (or  $\mu_{eff}$ ) [21][29], the values of effective material parameters such as permittivity ( $\epsilon_{eff}$ ) and permeability( $\mu_{eff}$ ) can be obtained using the values of susceptibilities as given in the Eq. (3.5) and (3.6). In the Eq. (3.3), (3.4)  $k_0$  is wavenumber given by  $k_0=\omega\sqrt{(\epsilon_0\mu_0)}$  and in Eq. (3.5), (3.6)  $d$  is the unit cell size

$$\chi_{es} = 1 + \frac{2j(S_{11}-1)}{\kappa_0(S_{11}+1)} \quad (3.3)$$

$$\chi_{ms} = 1 + \frac{2j(S_{11}+1)}{\kappa_0(S_{11}-1)} \quad (3.4)$$

$$\epsilon_{eff} = 1 + \frac{x_{es}}{d} \quad (3.5)$$

$$\mu_{eff} = 1 + \frac{x_{ms}}{d} \quad (3.6)$$

Normalized impedance  $Z_{nor}$  is given by Eq. (3.7).

$$Z_{nor} = \sqrt{(\mu_{eff} / \epsilon_{eff})} \quad (3.7)$$

### 3.3. RESULTS AND DISCUSSION

The MA unit cell's design structure is simulated, and the results are produced. Fig. 3.2(a) shows a three-dimensional model of the proposed unit cell and its corresponding absorptivity is shown in Fig. 3.2(b).

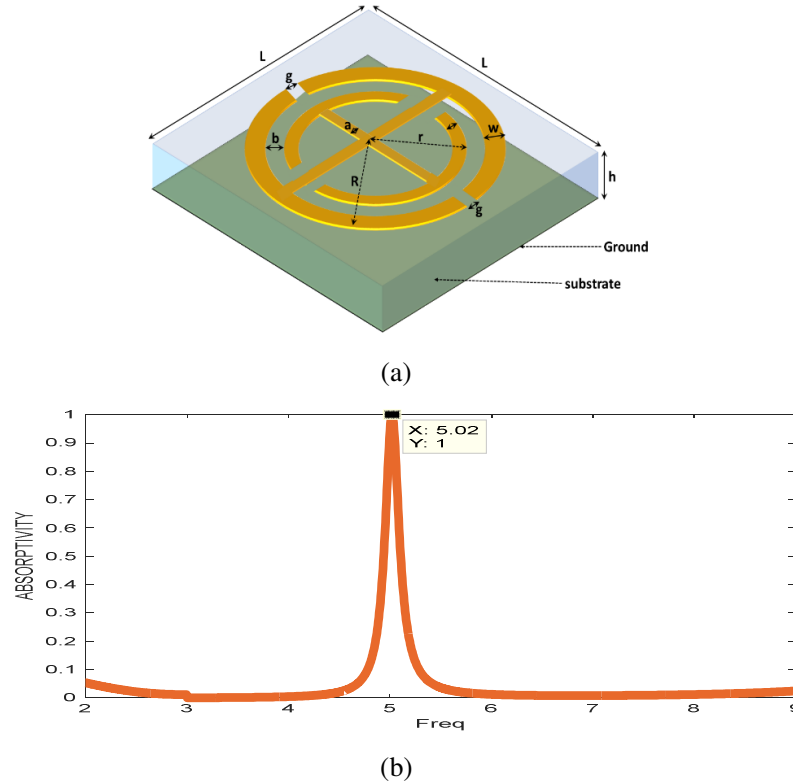


Fig. 3.2. (a) Three-dimensional geometrical model of the unit cell, (b) Simulated absorptivity plot under normal incidence and TE polarization.

It is observed from Fig. 3.2(b), the absorptivity is greater than 99% at around 5.02 GHz implies that the structure is a perfect conductor at around 5.02 GHz. Although the structure shows a narrowband absorption. Electric and magnetic fields are strongly in resonance and near-perfect impedance-matched to free space is obtained at around 5.02 GHz, resulting in near-zero reflection as seen in Fig. 3.3(c). Fig. 3.3(a) and 3.3(b) depicts the  $\epsilon_{\text{eff}}$  and  $\mu_{\text{eff}}$  respectively. The value of permittivity ( $\epsilon_{\text{eff}}$ ) at 5.02 GHz is  $1.023+j2.376$  and the value of permeability ( $\mu_{\text{eff}}$ ) is  $0.9773+j2.364$ , which are almost equal thus resulting in very low value of reflectivity and high absorptivity. The normalized impedance is near unity at 5.02 GHz ( $Z_{\text{nor}}=0.9974-j0.0095$ ) ( $|Z_{\text{nor}}| = 0.9945$ ) as shown in Fig. 3.3(c), resulting in very good impedance match with the free space impedance.

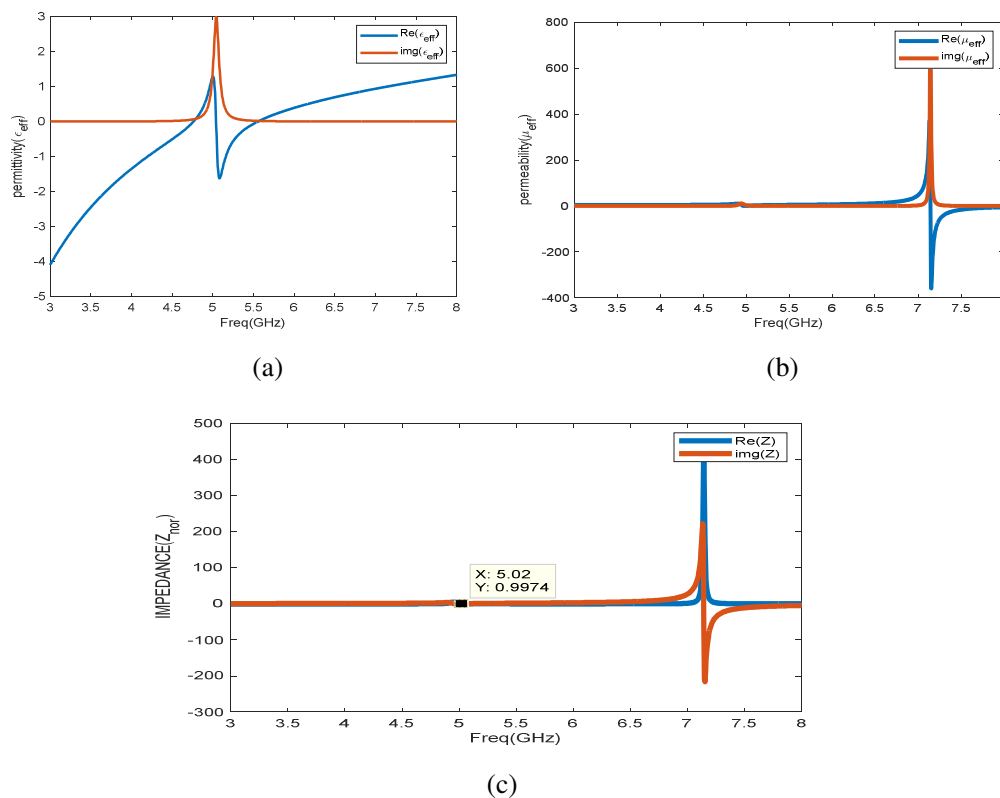


Fig. 3.3. Simulated results of (a) effective permittivity, (b) effective permeability and (c) Normalized impedance

The structure has been investigated under various polarization angles to demonstrate the proposed absorber's polarization behavior. The polarization angles ( $\phi$ ) have been varied from  $0^\circ$  to  $45^\circ$  in steps of  $15^\circ$  as shown in Fig. 3.4(a). It is observed that the absorptivity slowly decreases at 5.02 GHz with increasing polarization angle but also increases at around 8.8 GHz. The proposed MA structure has also been examined for



different values of oblique incidence angle ( $\Theta$ ) from  $0$  to  $60^\circ$  as shown in Fig. 3.4(b), the absorptivity remains almost constant up to  $30^\circ$  at around  $5.02$  GHz, with increasing the structures starts to show dual-band characteristics.

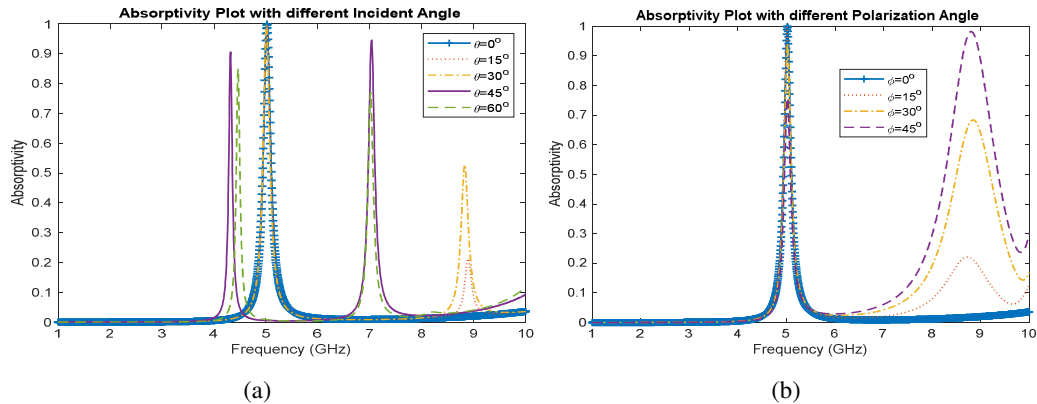


Fig. 3.4. Simulated Absorptivity results (a) for different incidence angle under TE polarization and (b) for different polarization angle under normal incidence.

Further, the absorptivity of the structure has been investigated under variation of the ring width size ( $w$ ) and the split gap size ( $g$ ) of the outer ring. The simulated results are shown in Fig. 3.5(a) and (b). It is observed from Fig. 3.5(a) that the absorptivity of the structure remains above 90% for different value of ' $w$ ' with a slight variation in center frequency can be observed. In the Fig. 3.5(b) it can be seen that for  $g=0.1$  mm absorptivity response shows two peak but with a very low absorptivity ( $\approx 70\%$ ). From  $g=0.2$  mm absorptivity response shows single absorption peak with resonant frequency increasing with increase in the split size ( $g$ ). It can be due to the change in the capacitance of the structure.

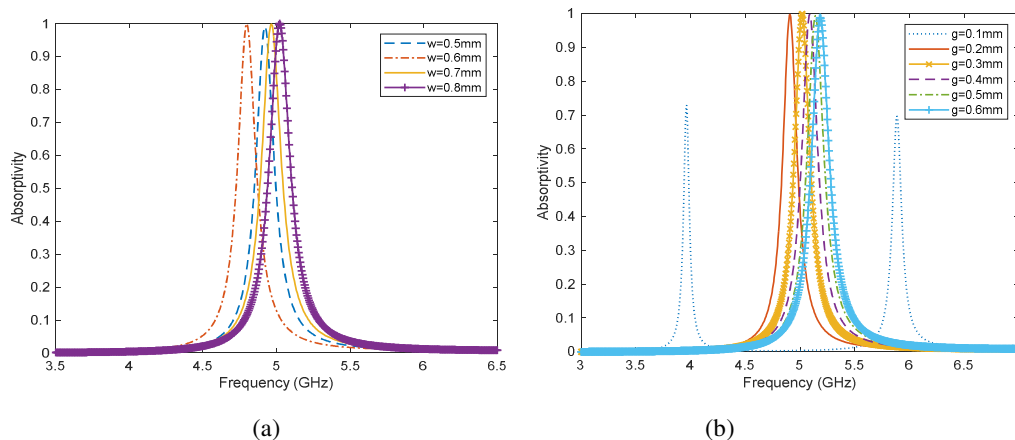


Fig. 3.5. Simulated Absorptivity variation w.r. to variation of (a) circular ring width and (b) outer ring split gap size

**TABLE - 3.2***Absorptivity results w.r.to different ring width*

Ring width (w)	Absorptivity (%)	Frequency (GHz)
0.5 mm	99.87	4.795
0.6 mm	99.11	4.92
0.7 mm	99.87	4.965
0.8 mm	99.99	5.02

**TABLE - 3.3***Absorptivity results w.r.to different outer ring split size*

Split Size (g)	Absorptivity (%)	Frequency (GHz)
0.1 mm	72.9, 69.72	3.965, 5.88
0.2 mm	99.72	4.91
0.3 mm	99.99	5.02
0.4 mm	99.82	5.09
0.5 mm	99.43	5.14
0.6 mm	98.84	5.18

### 3.4. ROTATED UNIT CELL

Further, to observe and study the effect of rotational angle of the splits of circular rings on the absorptivity response, we have rotated the structure  $45^\circ$  clockwise. Earlier the split in the outer ring was in perpendicular direction of the E-field and parallel to the H-field after the rotation the split is make  $45^\circ$  angle i.e., there was only electric excitation.

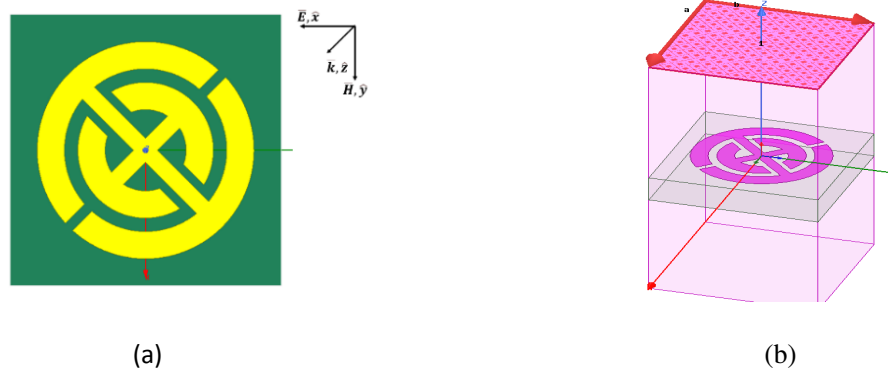


Fig. 3.6. (a) Proposed unit cell structure after  $45^\circ$  rotation, (b) simulation setup of the unit cell

**TABLE - 3.4***Comparison of MA structure with different angle of rotation*

Rotation	Absorptivity	Frequency (GHz)	Permittivity ( $\epsilon_{eff}$ )		Permeability ( $\mu_{eff}$ )		Normalized impedance ( $Z_{nor}$ )	
			Real ( $\epsilon_{eff}$ )	Imaginary ( $\epsilon_{eff}$ )	Real ( $\mu_{eff}$ )	Imaginary ( $\mu_{eff}$ )	Real ( $Z_{nor}$ )	Imaginary ( $Z_{nor}$ )
<b>0°</b>	99.99 %	5.02	1.023	j2.376	0.9773	j2.364	0.9975	-j0.0095
<b>45°</b>	99.8%	13.03	1.065	j0.8667	0.9298	0.9539	1.044	-j0.078

The structure is simulated and results are obtained. Figure 3.7 depicts the absorptivity response following rotation. The rotated structure now shows three different major absorptivity peaks with absorptivity greater than 90% at 8.83, 10.67, 13.03 GHz with 98.3%, 98.9%, 99.8% absorptivity respectively. Also the absorptivity response of the rotated structure now have a broadband absorption with a 1.92GHz bandwidth between frequency range of 11.88 GHz to 13.8 GHz with absorptivity more than 90%. The three different absorption peak can be due to the electric excitation of the outer ring, inner ring and the inner metallic cross resonator having resonance at different frequencies.

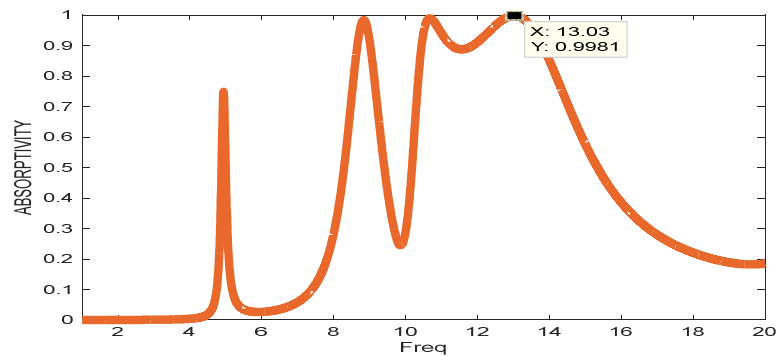
*Fig. 3.7. Simulated Absorptivity response of the rotated unit cell*

Fig. 3.8(a) depicts the effective permittivity ( $\epsilon_{eff}$ ) and permeability ( $\mu_{eff}$ ) and normalized impedance ( $Z_{nor}$ ) is shown in Fig. 3.8(b). The values of  $\epsilon_{eff}$  and  $\mu_{eff}$  at 13.03 GHz is  $1.065+j0.8667$  and  $0.9298+j0.9539$  respectively both are almost equal in magnitude, resulting in approximately unity normalized impedance ( $Z_{nor} = 1.044-j0.078$ ,  $|Z_{nor}| = 1.09$ ) therefore having very low reflectivity. To show the polarization behaviour of the structure and effect on absorptivity under varied incidence angles, the

rotated structure is further examined for varied incidence angles under TE polarisation and different polarization angles under normal incidence. Fig. 3.9(a) depicts the absorptivity response with different polarization angle and Fig. 3.9(b) depicts the absorptivity response under different incidence angle.

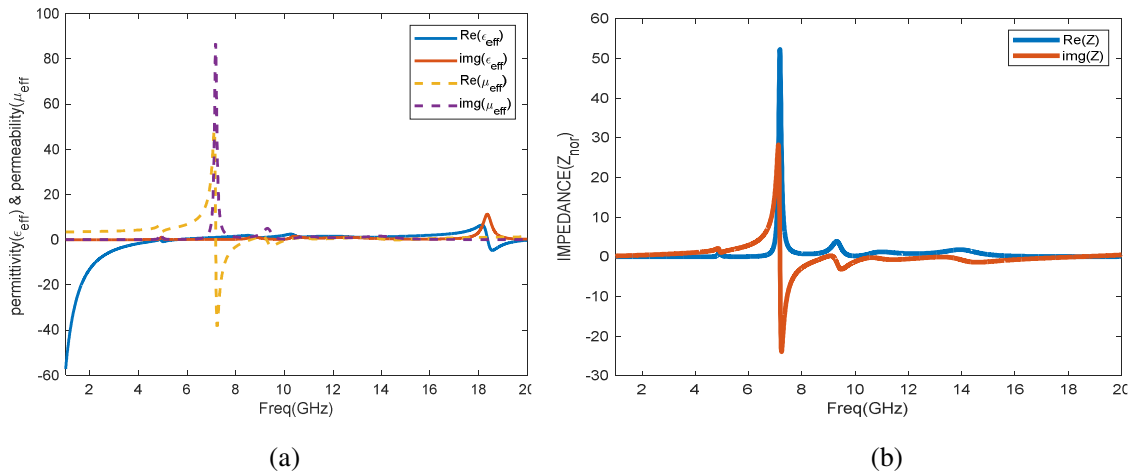


Fig. 3.8. Simulated results of (a) Permittivity and permeability (b) Normalized Impedance

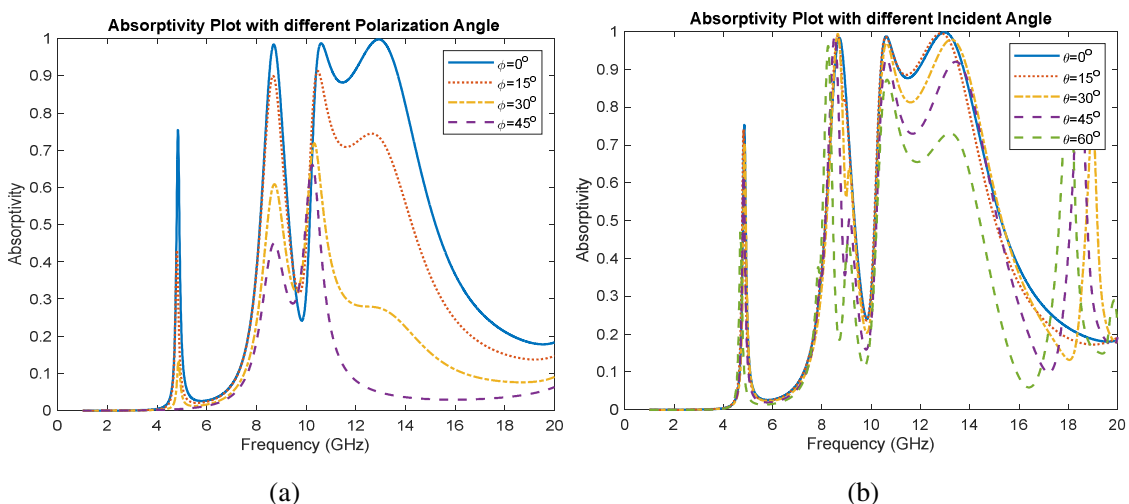


Fig. 3.9. Simulated Absorptivity of rotated structure (a) for different polarization angle under normal incidence and (b) for different incidence angle under TE polarization

Comparing the non-rotated structure with the one with  $45^{\circ}$  rotation, the later shows multiband absorption response in X-band and  $K_u$ -band, while the earlier one shows the near-unity absorptivity at 5.02 GHz in C-band. Both the structure have excellent impedance matching with free space. The non-rotated structure have near-constant absorptivity upto  $30^{\circ}$  of incidence angle, on the other hand the absorption characteristics of the rotated structure under different incidence angle remains constant upto  $15^{\circ}$  then

starts to decrease gradually for higher incidence angle. From the results of the absorptivity response it can be observed from the result that the structure is polarization-

**TABLE - 3.5**

Comparison of the proposed work with previous works

<b>Absorber</b>	<b>Centre Frequency (GHz)</b>	<b>Absorptivity (%)</b>	<b>Thickness (mm)</b>	<b>Unit cell size (mm<sup>2</sup>)</b>	<b>Polarization insensitive</b>
Priyanka garg <i>et. Al.</i> [19]	3.5	98.5	1.6	10x10	Yes
Priyanka garg <i>et. Al.</i> [27]	5.5	98.7	1	9x9	Yes
S. Ghosh <i>et. Al.</i> [24]	11.18	99.92	2	7.1x7.1	No
Cheng, Y <i>et. Al.</i> [26]	10.91	99	0.4	6x6	Yes
Proposed	5.02	99.99	1.6	8x8	No

dependent. The absorptivity of both the structure is maximum for normal incidence and  $0^\circ$  polarization angle for TE polarization. The earlier structure offer high absorptivity at narrowband the later one offer an advantage of multiband absorption. The applications for both structure on the demand of the application and the operational frequency. The non-rotated structure can find its application in wireless communication, radars, Wi-Fi etc. While the rotated structure wavelength selected radiators, P2P microwave radio links etc.

**CHAPTER - 4**

**Design and Analysis of Ring**

**Multiband Metamaterial Absorber**

---

## 4. DESIGN AND ANALYSIS OF RING MULTIBAND METAMATERIAL ABSORBER

This chapter demonstrates a metamaterial absorber (MA) inspired from a split-ring structure that exhibits three resonant peaks in the C-band and starting of X-band range. Proposed structure for the absorber is a three-layer rectangular split-ring with different absorption peaks at 8.488, 8.02, 7.51 GHz with 99.25%, 95.11%, 93.93% absorptivity respectively. MA is designed on a low-cost FR4 material with a substrate thickness 0.5 mm. Performance of the absorber is evaluated in terms of absorptivity related to three layers, material parameters and normalized impedance.

### 4.1. DESIGN AND SIMULATION

Suggested MA unit cell is a symmetrical structure composed of three metallic loops and a ground plane. All the three metallic strips are separated by a dielectric with a thickness of 0.5 mm making the structure with total thickness of 1.5 mm. The metal used is copper. Floquet Port and periodic boundary conditions are used to simulate the MA structure in Ansys HFSS. Fig. 4.1 shows a 3-D schematic of three-layer MA structure. The simulated result of reflection coefficient ( $S_{11}$ ) is shown in Fig. 4.2. It is observed from Fig 4.2 that there is a sharp decline in value of  $S_{11}$  at around 5GHz with a minimum value of  $S_{11}$  is -40.11 dB at 5.04 GHz.

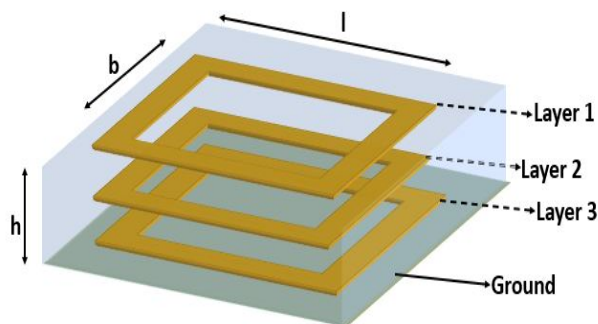


Fig. 4.1. Geometry of three-layer MA unit Cell

As observed in Fig. 4.3, structure has 99.99% absorptivity at 5.04 GHz. It is observed that there is also a another minor absorption peak at around 5.4 GHz with 95% absorptivity and later absorption capability of structure starts to decline on the higher frequencies. It can be interpreted from the Fig. 4.3 that MA structure is perfect absorber at 5.04 GHz and shows absorptivity more than 90% at 5.4GHz.

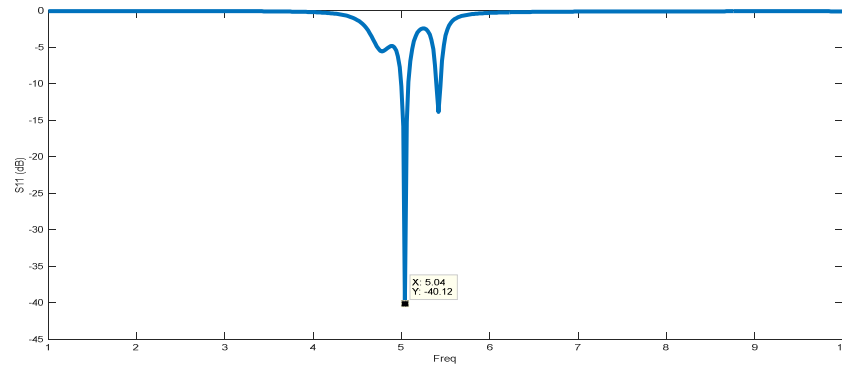


Fig. 4.2. Plot of  $S_{11}$  w.r.to frequency (GHz)

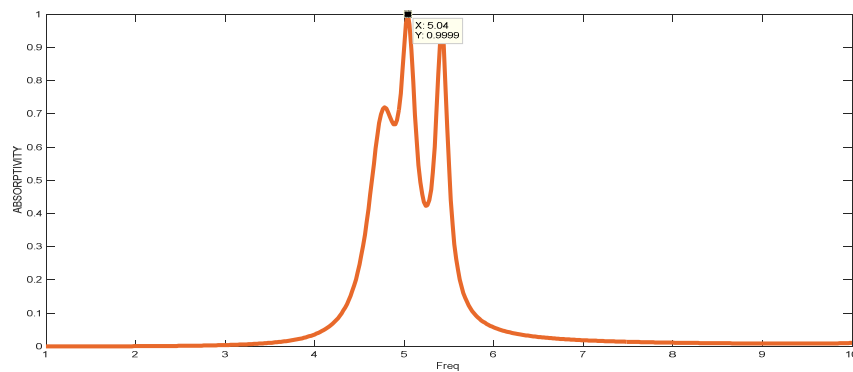


Fig. 4.3. Absorptivity result of MA unit cell

To design a split-ring MA, we have to introduce a slots in the middle of one side of metallic rings of each layers of the MA. Thus, the final structure will resembles to a split ring structure.

In the first stage, a 1mm wide slot has been introduced in the middle of one side on the top layer of the ring structure, such that the slot will be normal to the incident electric field therefore it is electrically excited. Since the edges of the slot will normal to incidence E-field of electromagnetic fields, electrons in the metal will experience a force in opposite direction of the applied electric field resulting in accumulation of positive and negative charges on the opposite edges of the slot. Thus a capacitance will be formed i.e., the slot will act as a capacitor. Since the rings are made from metal it will have some inductance. Thus a single metallic split-ring layer will act as an LC circuit. Corresponding split ring structure is shown in Fig. 4.4.



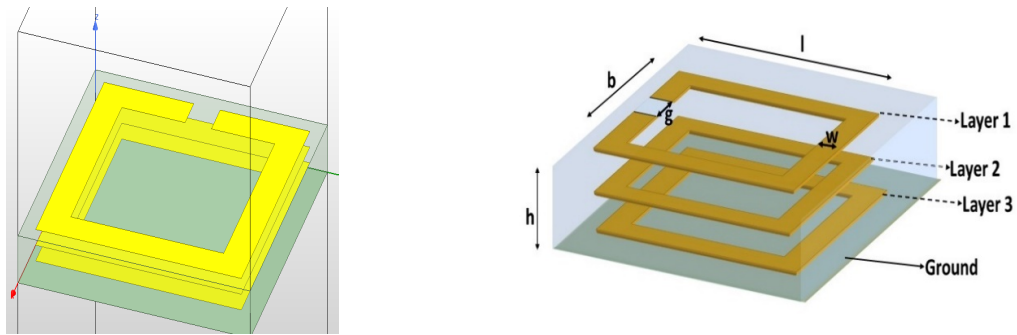


Fig. 4.4. Geometry of a 3-layer MA with a slot on top layer

The reflection coefficient ( $S_{11}$ ) plot has been depicted in the Fig. 4.5. It has been observed from the Fig. 4.5 that the reflection coefficient is less than -10 dB at around 5.03 GHz and 8.48 GHz and with a minimum value of -20.7 dB at 5.03 GHz which is the operational frequency of this structure. It is also observed from the Fig. 4.6 that in comparison with the original structure the absorptivity plot now shows multiple peaks with two significant peaks with 99.16 % and 94.64 % at 5.03 and 8.488 GHz respectively. The results shows that due to multiple layer structure multi frequency resonance is obtained in MA.

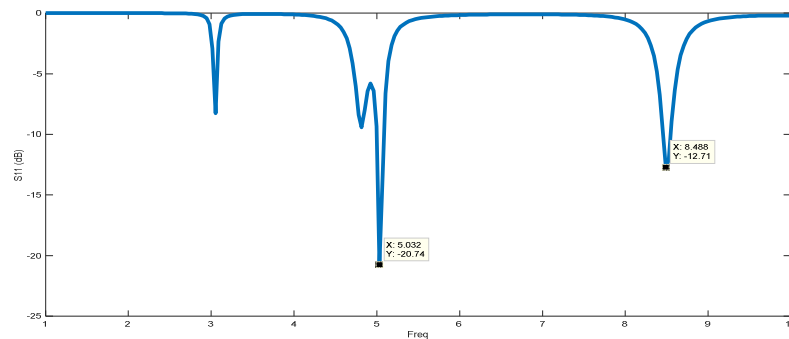


Fig. 4.5. Plot of  $S_{11}$  vs frequency of MA unit cell with one slot

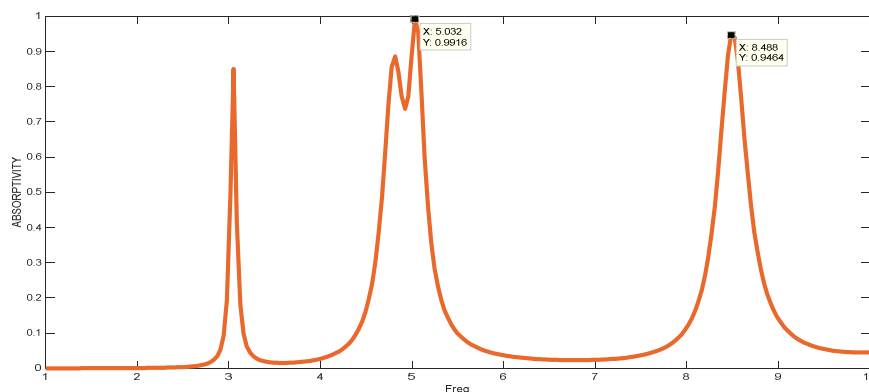


Fig. 4.6. Absorption result of the MA unit cell with a slot

In the second stage, in addition with the first slot in the top layer, another slot has been introduced in the middle layer. The slot in the middle has same dimension as on the top layer and it is exact below the top layer slot. As depicted in Fig. 4.7, the structure now consists of slots on the top layer as well as on the middle layer. Corresponding absorptivity curve is shown in Fig. 4.8. With the two slots in the layers, resonance frequency shift has been observed and corresponding three significant absorption peaks at 3.19, 4.81, 8.45 GHz with 99.93 %, 98.26 %, 96.67 % absorptivity respectively has been achieved. It is also observed from the fig. 4.8 that absorptivity has been increased with the increase in the slots.

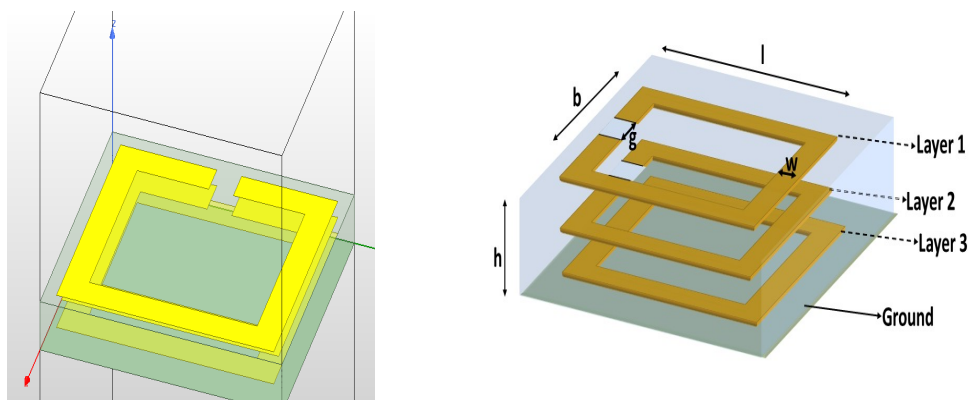


Fig. 4.7. Geometry of MA unit cell with 2 slots in layers

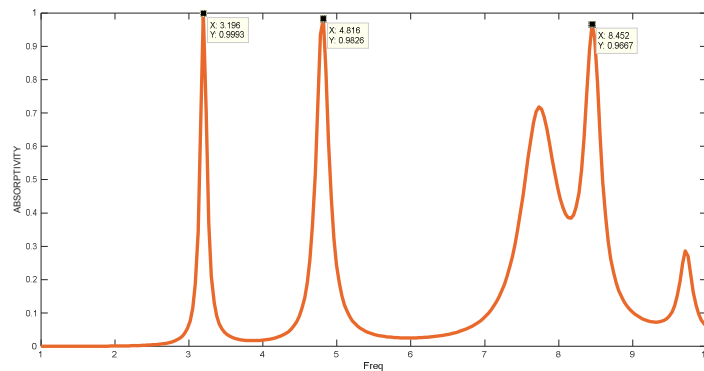


Fig. 4.8. Absorption plot of unit cell with slots in the middle and top layer.

In third stage, a three-layer split ring MA structure have made by introducing another 1mm wide slot in the bottom layer so as to make all three layers as a split ring. A schematic diagram of three-layer split ring structure is shown in Fig. 4.9(a). Fig. 4.9(b) shows top view of the split-ring structure.

As depicted in Fig. 4.10, the split ring MA unit cell shows different absorption peaks at 8.488, 8.02, 7.51 GHz with 99.25%, 95.11%, 93.93% absorptivity respectively. All the major frequency points are at very close interval. It can be observed that MA unit cell have absorptivity greater than 90% for multiple frequency.

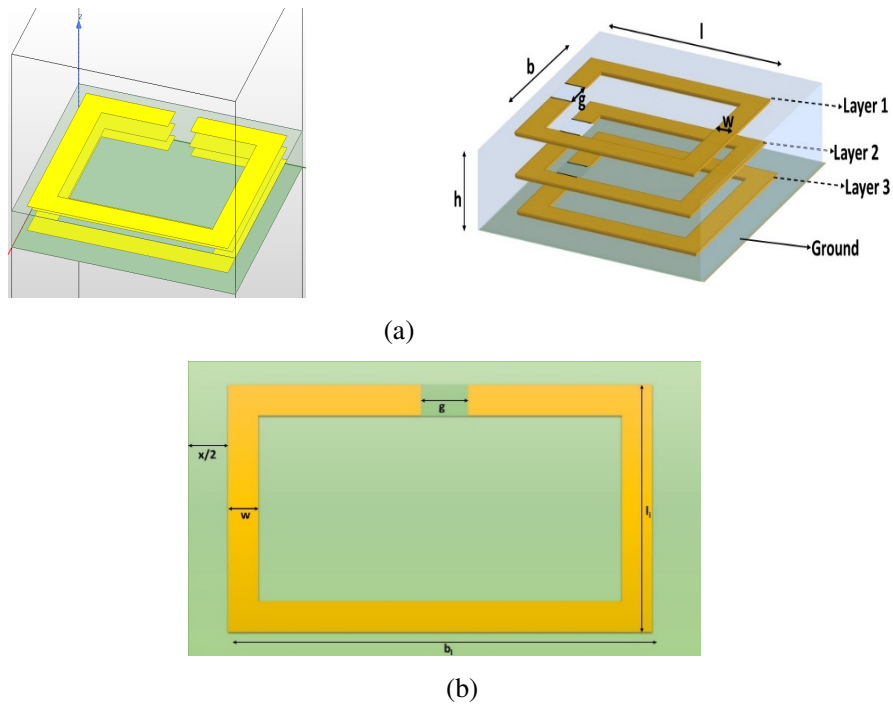


Fig. 3.9. Geometry of (a) three-layer split ring MA unit cell (b) Top view of the unit cell

It can also be observed from the Fig. 4.10 that the structure is now showing a broadband absorption instead showing multiple absorption peaks at different frequencies lying in two band C-band and X-band therefore, the structure is a multiband structure.

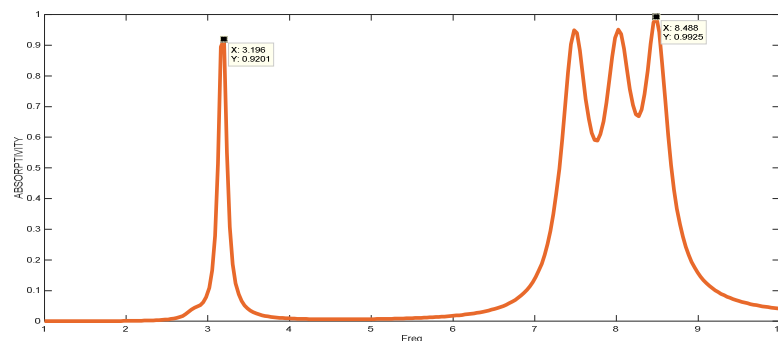


Fig. 4.10. Absorptivity result of split ring MA unit cell.

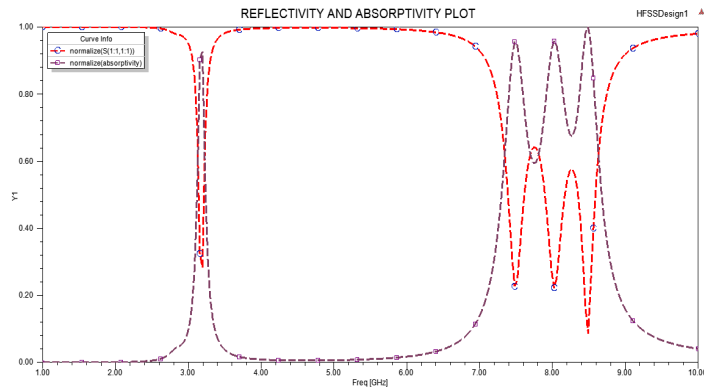


Fig. 4.11. Simulated results of reflectivity and absorptivity of split-ring unit cell.

Fig. 4.11 shows the reflection coefficient( $S_{11}$ ) and absorptivity curves. It can be observed from the Fig. 4.11 that the absorptivity approaches near unity when the reflection approaches near zero. The design parameters of the final unit cell with slits are as follows:

**TABLE - 4.1**

*Design Parameters of the unit cell*

PARAMETER	VALUE	DESCRIPTION
<b>H</b>	1.5 mm	Substrate Height (three layers)
<b>B</b>	8.8 mm	Metal loop width
<b>W</b>	1 mm	Metal loop size
<b>X</b>	1 mm	Distance along b
<b>G</b>	1 mm	Slot gap size

**TABLE - 4.2**

*Length and size of metal loops*

	$L_1$	$W_1$
<b>Layer - 1</b>	7.8 mm	1 mm
<b>Layer - 2</b>	7.2 mm	1.2 mm
<b>Layer - 3</b>	7.8 mm	1 mm

A comparison of all the structure's absorptivity plots is shown in Fig. 4.12. It can be observed that final three-layer split-ring structure shows multiband absorption characteristics with three distinct absorption peaks having absorptivity greater than 90%. The first structure without any slot shows only one absorption peak and after introduction of the slots MA starts showing multiband absorption. The operating frequency is also been shifted from 5.04 GHz to 8.48 GHz in the final structure.

**TABLE - 4.3**

*Absorptivity results with different numbers of slots*

No. of slots	Frequency (GHz)	Absorptivity
0	5.04	99.99 %
1	5.03	99.16 %
	8.48	94.64 %
2	3.19	99.93 %
	4.81	98.26 %
	8.45	96.67 %
3	7.51	93.93%
	8.02	95.11%
	8.48	99.25 %

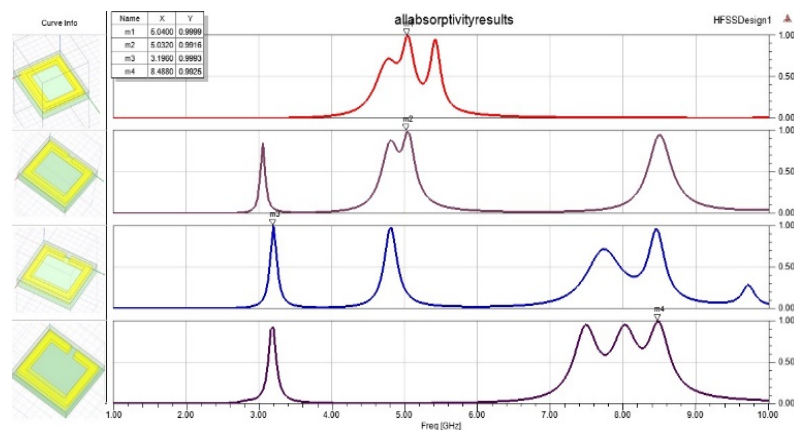


*Fig. 4.12. Comparison of absorptivity of all structures*

## 4.2. PARAMETRIC ANALYSIS

Further the effect of varying slot width ( $g$ ) on absorptivity of the structure is studied in this section. Multiple values of slot width ( $g$ ) have been taken such as 0.5, 0.75, 1, 1.25, 1.5 mm. The simulated results variation of parameter ' $g$ ' on absorptivity is shown in the Fig. 4.13. The Multiband absorption characteristics remain same but with a slight change in operational frequency having maximum absorption. Varying the slot width changes the structure's capacitance and inductance when considering the structure as RLC circuit which therefore leads to the change in operating frequency.

**TABLE – 4.4**

*Absorptivity results with different slot size*

SLIT WIDTH (g)	ABSORPTIVITY	FREQUENCY (GHZ)
0.5 mm	99.43 %	7.73
0.75 mm	99.14 %	8.36
1 mm	99.25 %	8.48
1.25 mm	97.98 %	8.48
1.5 mm	99.85 %	7.66

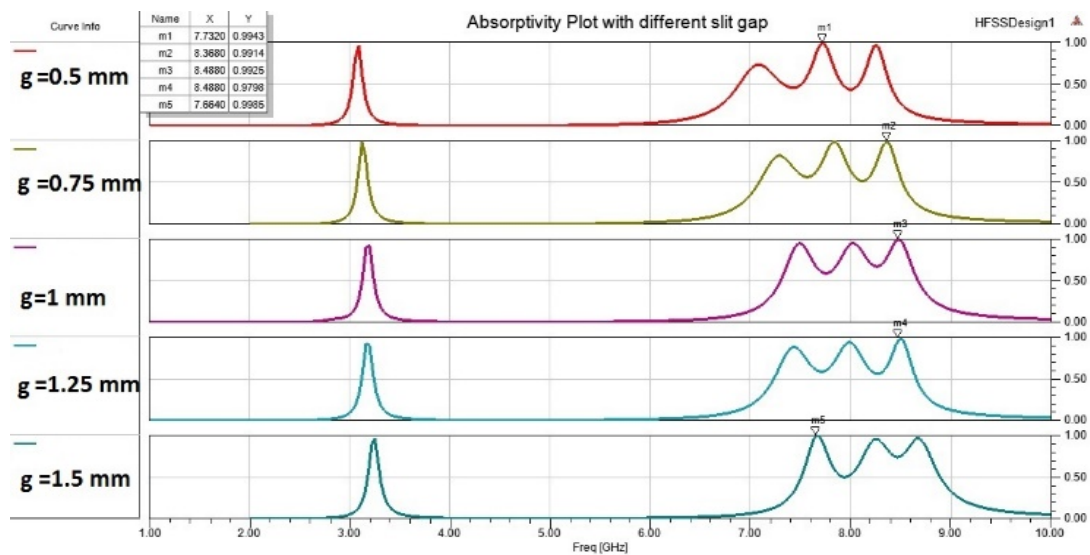


*Fig. 4.13. Absorptivity variation with variation of slot size*

**CHAPTER – 5**  
**CONCLUSION**

---

## 5.1. CONCLUSION

This report presents the application of metamaterials as electromagnetic absorbers. The design techniques and their analysis of metamaterials absorbers has been discussed. The structures presented are low-cost and simple in design, making them ideal for practical applications.

In Chapter 3, a novel single layer ultrathin metamaterial absorber based on dual circular split-ring cross-resonator with resonant frequency of 5.02 GHz has been proposed. The proposed structure consists of two concentric circular split-ring with a cross shaped metallic strip in the middle of both the rings attached to them. The proposed structure offers near-unity absorptivity around 99.99% at desired frequency of 5.02 GHz. The effective permittivity, effective permeability are coming out to be approximately equal resulting excellent impedance matching. The absorptivity response of the structure is almost identical for different values of slot size and ring size. The proposed structure is found to be polarization dependent because of non-symmetrical geometry. Further, the effect of rotational angle of the splits have also been analyzed by the rotating the structure 45° clockwise. The absorptivity is greater than 90% at three frequencies i.e., 8.83, 10.67, 13.03 GHz with 98.3%, 98.9%, 99.8% absorptivity respectively and it also have a wideband absorption response with 1.92 GHz bandwidth between frequencies range of 11.88 GHz to 13.8 GHz with absorptivity greater than 90%. It was found that the proposed structure is not polarization independent. The proposed absorber can find its various field like wireless communication, radars, WiFi etc.

In chapter 4, a three-layer split-ring metamaterial absorber (MA) unit cell has been proposed. The split-ring MA unit cell is being derived from a conventional three-layer ring MA structure by introducing slots in the metallic loops of the structure. The three-layer structure is a signal resonance frequency structure with 99% absorptivity at 5.04 GHz. It is observed from the simulated results that by introducing slots in the MA cell, it behaves as a multiband electromagnetic absorber. The split-ring MA cell shows multiband absorption with absorption peaks at 8.488, 8.02, 7.51 GHz with 99.25%, 95.11%, 93.93% absorptivity respectively. Further, the effect of varying slot size on the absorptivity has also been studied and it has been observed that by changing the slot width only shift in the frequency can be obtained without any significant change in the absorptivity.



# **CHAPTER - 6**

## **FUTURE SCOPE**

---

## **6. FUTURE SCOPE**

Metamaterials based absorbers have tremendous future scope in the future because of their properties and applications. Metamaterial absorbers can be used with sensors for enhancing their sensitivity. New structures based on fractals can be designed. In the future the metamaterial absorbers can be designed for application in THz frequency regime for many applications such as sensing, infrared spectroscopy etc.

Polarization insensitive broadband metamaterials can be designed for various applications in communication devices. Metamaterials can also be integrated in MIMO devices to reduce mutual coupling between antennas.

The structure proposed in chapter 3 can be further enhanced for polarization insensitivity by having symmetrical geometry. It can be integrated with other structures for a broadband absorption. Further work can also be done by integrating the same structure with different rotational angles.

The second structure given in chapter 4 can be enhanced for more broadband response and it can be enhanced for a single layer structure.

---

## LIST OF PUBLICATIONS

1. Keshav Bhati, Priyanka Jain, **“DESIGN AND ANALYSIS OF A DUAL SPILTRING BASED METAMATERIAL ABSORBER,”** 12th International Conference on Computing, Communication and Networking Technologies (ICCCNT), 2021.
  2. Priyanka Jain, Keshav Bhati, **“DESIGN AND ANALYSIS OF RING MULTIBAND METMATERIAL ABSORBER,”** 6th International Conference on Communication and Electronics Systems (ICCES), pp. 432-437, 2021.
-

---

## REFERENCES

- [1]. V. G. Veselago, "The electrodynamics of substances with simultaneously negative values of  $\epsilon$  and  $\mu$ ", *Physics-Uspeski*, vol. 10, no. 4, pp. 509-514, 1968.
  - [2]. J. B. Pendry, A. J. Holden, D. J. Robbins, and W. J. Stewart, "Magnetism from conductors and enhanced nonlinear phenomena," *IEEE Transactions on Microwave Theory and Techniques*, vol. 47, no. 11, pp. 2075-2084, 1999.
  - [3]. D. R. Smith, Willie J. Padilla, D. C. Vier, S. C. Nemat-Nasser, and S. Schultz, "Composite Medium with Simultaneously Negative Permeability and Permittivity", *Phys. Rev. Lett.*, Vol. 84, no. 18, pp. 4184-4187, 2000.
  - [4]. Caloz, Christophe and Tatsuo Itoh, "Electromagnetic Metamaterials: Transmission line Theory and Microwave Applications: The Engineering Approach", *John Wiley & Sons, Inc*, 2006.
  - [5]. Priyanka garg (2020), "Design and Analysis of Metamaterial Based Microwave components", Ph. D. dissertation, Department of Electronics and Communication Engineering, Delhi Technological University, Delhi.
  - [6]. S. Ramo, J. R. Whinnery and T. Van Duzer, "Fields and Waves in Communication Electronics" (*New York: John Wiley & Sons, 1965*). pp. 51-53
  - [7]. Kushwaha, Nagendra & Kumar, Raj. (2014). "Study of different shape Electromagnetic Band Gap (EBG) structures for single and dual band applications," *Journal of Microwaves, Optoelectronics and Electromagnetic Applications*, Vol. 13, no. 1, pp. 16-30, 2014.
  - [8]. Y. Lee, J. Yeo, K. Ko, Y. Lee, W. Park, and R. Mittra, "A novel design technique for control of defect frequencies of an electromagnetic band gap (EBG) cover for dual band directivity enhancement", *Microw. Opt. Technol. Lett.*, vol. 42, no. 1, pp. 25-31, Jul. 2004.
  - [9]. M. Gil, J. Bonache, F. Martín, "Metamaterial filters: A review", *Metamaterials*, Vol. 2, Issue 4, 2008, pp. 186-197.
  - [10]. Statsenko, Lyubov G., et al. "Designing Microwave Filters Using Metamaterials." *Key Engineering Materials*, vol. 806, Trans Tech Publications, Ltd., June 2019, pp. 167-172.
  - [11]. J. B. Pendry, "Negative Refraction Makes a Perfect Lens," *Phys. Rev. Lett.*, vol. 85, no. 18, pp. 3966-3969, Oct. 2000.
  - [12]. D. Schurig, J. J. Mock, B. J. Justice, S. A. Cummer, J. B. Pendry, A. F. Starr, and D. R. Smith, "Metamaterial electromagnetic cloak at microwave frequencies," *Science*, vol. 314, pp. 977-980, 2006.
  - [13]. R. O. Ouedraogo, E. J. Rothwell, A. R. Diaz, K. Fuchi and A. Temme, "Miniaturization of patch antennas using a metamaterial-inspired technique," *IEEE Transactions on Antennas and Propagation*, vol. 60, no. 5, pp. 2175-2182, 2012.
-

- 
- [14]. X. Cheng, D. E. Senior, C. Kim, and Y. Yoon, "A compact omnidirectional self-packaged patch antenna with complementary split-ring resonator loading for wireless endoscope applications," *IEEE Antennas and Wireless Propagation Letters*, vol. 10, pp. 1532-1535, 2011.
- [15]. N. I. Landy, S. Sajuyigbe, J. J. Mock, D. R Smith, W. J and Padilla, "Perfect metamaterial absorber," *Phys. rev. lett.*, vol. 100, 2008.
- [16]. M.H.Li, L.Hua Yang, B.Zhou, X.Peng Shen, Q.Cheng, and T.J.Cui, "Ultrathin multiband gigahertz metamaterial absorbers," *Journal of Applied Physics*, Vol. 110, Issue 1, pp. 014909, 2011.
- [17]. H.Tao, N.Landy, C.M.Bingham, X.Zhang, R.D.Averit, and W.J.Padilla, "A metamaterial absorber for the terahertz regime: design, fabrication and characterization," *Optics Express*, Vol. 16, No. 10, pp. 7181-7188, May 2008.
- [18]. Junyi Ren, Shuxi Gong, "Low-RCS Monopolar Patch Antenna Based on a Dual-Ring Metamaterial Absorber" *IEEE Antennas and Wireless Propagation Letters*, vol. 17, no. 1, pp. 102-105, January 2018.
- [19]. Priyanka Garg and Priyanka Jain, "Analysis of a novel Metamaterial Absorber using equivalent circuit model operating at 3.5 GHz", *2020 IEEE International Conference on Computational Electromagnetics (ICCEM 2020)*, pp. 246-247, 2020.
- [20]. Min Zhong, "Design and measurement of a narrow band metamaterial absorber in terahertz range", *Optical Materials*, Vol. 100, 109712, 2020.
- [21]. Priyanka Garg, Priyanka Jain, "Novel ultrathin penta-band metamaterial absorber", *AEU - International Journal of Electronics and Communications*, Vol. 116, 2020, 153063.
- [22]. R.M.H. Bilal, M.A. Baqir, P.K. Choudhury, M.M. Ali, A.A. Rahim, W. Kamal, "Polarization insensitive multi-band metamaterial absorber operating in the 5G spectrum", *Optik*, Vol. 216, 2020, 164958.
- [23]. S. Bhattacharyya, S. Ghosh, D. Chaurasiya and K. V. Srivastava, "A broadband wide angle metamaterial absorber for defense applications," *2014 IEEE International Microwave and RF Conference (IMaRC)*, 2014, pp. 33-36.
- [24]. S. Ghosh, S. Bhattacharyya, D. Chaurasiya and K. V. Srivastava, "An Ultrawideband Ultrathin Metamaterial Absorber Based on Circular Split Rings," *IEEE Antennas and Wireless Propagation Letters*, vol. 14, pp. 1172-1175, 2015.
- [25]. Wen, Ding-e & Helin, Yang & Ye, Qiwei & Li, Minhua & Guo, Linyan & Zhang, Jianfeng. (2013). "Broadband metamaterial absorber based on a multi-layer structure". *Physica Scripta*, vol. 88, 015402, 2013.
- [26]. Cheng, Y., Yang, H., Cheng, Z. et al. "Perfect metamaterial absorber based on a split-ring-cross resonator". *Appl. Phys.*, vol. 102, pp. 99-103, 2011.
-

- [27].Priyanka Garg and Priyanka Jain, “Isolation Improvement of MIMO Antenna Using a Novel Flower Shaped Metamaterial Absorber at 5.5 GHz WiMAX Band”, *IEEE transactions on circuits and systems—ii: express briefs*, vol. 67, no. 4, 2020
- [28]. Saxena, Gaurav & Awasthi, Yogendra & Jain, Priyanka, “Design of meta surface absorber for low RCS and high isolation MIMO antenna for radio location & navigation”, *AEU - International Journal of Electronics and Communications*. Vol. 133, 153680, 2021.
- [29].Holloway CL, Kuester EF, Dienstfrey A. “Characterizing metasurfaces/metafilms: the connection between surface susceptibilities and effective material properties”. *IEEE Antennas Wireless Propagation Lett.*,
- [30]. S.R. Thummaluru, N. Mishra, and R. K. Chaudhary, “Design and analysis of an ultrathin X-band polarization-insensitive metamaterial absorber,” *Microwave and Optical Technology Letters*, vol. 58, no. 10, pp. 2481-2485, 2016.
- [31].S. Bhattacharyya, S. Ghosh, and K. V. Srivastava, “Triple band polarization independent metamaterial absorber with bandwidth enhancement at X-band” *Journal of Applied Physics*, vol. 114, no. 9, p. 094514, 2013.
-